Acta Biomaterialia xxx (xxxx) xxx

Contents lists available at ScienceDirect

Acta Biomaterialia

journal homepage: www.elsevier.com/locate/actabiomat

Full length article

Graphene oxide substrates with N-cadherin stimulates neuronal growth and intracellular transport

Ellen C. Qin [a], Mikhail E. Kandel [b,c], Evangelos Liamas [d], Tauseef B. Shah [e], Chaeyeon Kim [f], Collin D. Kaufman [c,g], Zhenyu J. Zhang [d], Gabriel Popescu [b,c], Martha U. Gillette [c,e,g], Deborah E. Leckband [c,f,*], Hyunjoon Kong [c,f,*]

[a] Department of Materials Science and Engineering, University of Illinois, Urbana-Champaign, United States
[b] Department of Electrical and Computer Engineering, University of Illinois, Urbana-Champaign, United States
[c] Beckman Institute for Advanced Science & Technology, University of Illinois, Urbana-Champaign, United States
[d] School of Chemical Engineering, University of Birmingham, Edgbaston, United Kingdom
[e] Department of Molecular and Integrative Physiology, University of Illinois, Urbana-Champaign, United States
[f] Department of Chemical and Biomolecular Engineering, University of Illinois, Urbana-Champaign, United States
[g] Neuroscience Program, University of Illinois, Urbana-Champaign, United States

ARTICLE INFO

Article history:
Received 12 October 2018
Received in revised form 12 March 2019
Accepted 1 April 2019
Available online xxxx

Keywords:
Neurons
Cadherin
Graphene oxide
Reduced graphene oxide
Intracellular transport

ABSTRACT

Intracellular transport is fundamental for neuronal function and development and is dependent on the formation of stable actin filaments. N-cadherin, a cell–cell adhesion protein, is actively involved in neuronal growth and actin cytoskeleton organization. Various groups have explored how neurons behaved on substrates engineered to present N-cadherin; however, few efforts have been made to examine how these surfaces modulate neuronal intracellular transport. To address this issue, we assembled a substrate to which recombinant N-cadherin molecules are physiosorbed using graphene oxide (GO) or reduced graphene oxide (rGO). N-cadherin physisorbed on GO and rGO led to a substantial enhancement of intracellular mass transport along neurites relative to N-cadherin on glass, due to increased neuronal adhesion, neurite extensions, dendritic arborization and glial cell adhesion. This study will be broadly useful for recreating active neural tissues *in vitro* and for improving our understanding of the development, homeostasis, and physiology of neurons.

Statement of Significance

Intracellular transport of proteins and chemical cues is extremely important for culturing neurons *in vitro*, as they replenish materials within and facilitate communication between neurons. Various studies have shown that intracellular transport is dependent on the formation of stable actin filaments. However, the extent to which cadherin-mediated cell–cell adhesion modulates intracellular transport is not heavily explored. In this study, N-cadherin was adsorbed onto graphene oxide-based substrates to understand the role of cadherin at a molecular level and the intracellular transport within cells was examined using spatial light interference microscopy. As such, the results of this study will serve to better understand and harness the role of cell–cell adhesion in neuron development and regeneration.

Abbreviations: GO, graphene oxide; rGO, reduced graphene oxide; N-cad, N-cadherin; N-cadherin-glass, glass physiosorbed with N-cadherin-Fc; N-cadherin-GO-glass, glass coated with GO flakes and physiosorbed with N-cadherin; N-cadherin-rGO-glass, glass coated with rGO flakes and physiosorbed with N-cadherin; SLIM, spatial light interference microscopy; MAP2, microtubule associated protein 2; GFAP, glial fibrillary acidic protein.

* Corresponding authors at: Department of Chemistry, University of Illinois, 600 South Mathews Avenue, 127 RAL, Box C-3, Urbana, IL 61801, United States (D.E. Leckband). Department of Chemical and Biomolecular Engineering, University of Illinois, 600 South Mathews Avenue, RAL 108, Urbana, IL 61801, United States (H. Kong).

E-mail addresses: leckband@illinois.edu (D.E. Leckband), hjkong06@illinois.edu (H. Kong).

https://doi.org/10.1016/j.actbio.2019.04.005
1742-7061/

1. Introduction

The intracellular transport of synaptic vesicle precursors, neurotransmitter and neurotrophic factors, proteins and mRNA is fundamental for the function, survival, and morphogenesis of neurons. Motor proteins bidirectionally transport cargoes containing various membrane organelles and protein complexes along the axons and dendrites. The transport of molecules and organelles from the cell body to the synapses or cell membrane is referred to as anterograde transport, whereas the opposite is referred to as retrograde transport. For instance, a variety of newly synthesized proteins such as actin and neurofilaments are produced in the cell body and transported along the cytoskeleton filaments to the neuronal membrane to form and maintain axons that are involved in communication with neighboring and distant cells [1]. On the other hand, neurotrophic factors which are crucial to neuronal survival, such as nerve growth factor (NGF), bind to the membrane-associated receptors, are internalized, and actively transported to the cell body [2].

Impairment of intracellular transport has often been linked to neurodegenerative diseases. Genetic mutations in Alzheimer's disease, for example, alters the roles of several proteins involved in trafficking cargo inside nerve cells, and the disruption of intracellular transport due to the protein defects results in cell death [3,4]. Similar impairments in intracellular transport have also been linked to Parkinson's disease, amyotrophic lateral sclerosis (ALS), and hereditary spastic paraplegia [5]. Defective transport can arise from various mechanisms, including the destabilization of microtubules, impairment of motor protein attachment to the microtubules, and/or altered kinase activities [6]. As a result, the formation of stable actin filaments, which form tracks for motor proteins to transport cargos, is extremely important for proper intracellular transport [7].

Various extracellular matrix and cell–cell adhesion proteins are involved in the formation of the actin cytoskeleton. Cadherins, in particular, are cell–cell adhesion proteins which associate with catenin and interact with the actin cytoskeleton [8–10]. N-cadherin is essential for the functional organization of adult neural tissue and the development of neural networks by mediating axon guidance [11], neurite outgrowth [12–14], dendritic arborizations [9], and synaptogenesis [15,16], all of which require actin polymerization at the growth cones [17]. In addition, studies demonstrate that the function of N-cadherin can be recapitulated *in vitro* [18]. For example, recombinant N-cadherin protein coated onto various surfaces has been shown to mediate neurite outgrowth of neurons [14,19]. Approaches to improve the function of N-cadherin exploit either the use of an adhesive peptide motif for N-cadherin [20–22] or the use of engineered epitopes to bind and orient cadherin extracellular domains on different substrates [23–25]. Until now, current studies have primarily focused on understanding how neurons interact with N-cadherin coated surfaces in terms of neurite outgrowth; [14,23,24,26]; however, to our knowledge, no studies have examined how N-cadherin mediated interactions between neurons and N-cadherin coated surfaces affects intracellular transport thus far. In addition, the exact nature of neuronal interactions on N-cadherin coated GO compared to rGO is still unknown.

In recent years, a quantitative phase imaging technique called spatial light interference microscopy (SLIM) has been developed for non-invasive and label-free imaging of the intracellular mass transport within cells [27–31]. Using SLIM, the optical path length differences in the neuronal cell body and neurites due to intracellular mass transport can be observed and quantified [28,32]. SLIM is an improvement from the conventional phase contrast imaging, in which the halo artifact from phase contrast imaging overestimates the neuronal cell size and prevents quantitative information about the intracellular mass transport [33]. Moreover, SLIM offers an opportunity to monitor the intracellular transport non-invasively over multiple days. Using SLIM, it has been demonstrated that inhibitors and neuronal densities strongly affect intracellular transport in neurons [28,31]. For this study, SLIM allows the ability to examine how N-cadherin mediated interactions between neurons and N-cadherin coated surfaces affects intracellular transport.

Recently, graphene oxide (GO) and reduced graphene oxide (rGO) have been shown to promote protein adhesion and support neuronal function [34–36]. For instance, graphene functionalized with poly-lysine has been shown to significantly enhance neurite numbers and lengths in hippocampal neurons [35]. Graphene functionalized with laminin also enhances the differentiation of neural stem cells to neurons [37]. Gonzalez-Mayorga et al. recently demonstrated poly-lysine and N-cadherin can be coated onto microfibers made of rGO through non-covalent interactions and chemical means using carbodiimide chemistry. The resulting microfiber has been shown to improve neural growth in injured central neural tissue [26]. In addition, Lee et al. showed that insulin interacts with graphene differently than GO. The resulting changes in protein conformation is attributed to varying degrees of non-covalent interactions. In turn, insulin when bound to graphene or GO affects stem cell growth and differentiation differently [38]. This study demonstrated the importance of investigating the effects of both GO and rGO on protein adsorption and cellular interactions.

To regulate the cytoskeleton formation and subsequent intracellular transport, we hypothesized that adsorbing N-cadherin onto graphene-based substrates will enhance the growth and intracellular transport of hippocampal neurons. We tested this hypothesis by adsorbing recombinant N-cadherin extracellular domains onto uncoated glass or onto glass coated with either GO or rGO flakes. The adhesivity of N-cadherin layers on GO or rGO coated glass and the number of N-cadherin bound to the different substrates was evaluated by atomic force microscopy (AFM) and enzyme-linked immunosorbent assay (ELISA), respectively. In parallel, the secondary structure of adsorbed N-cadherin on GO or rGO flakes was examined using circular dichroism spectroscopy. Primary rat hippocampal neurons were seeded on the N-cadherin ectodomain coupled to uncoated and coated glass substrates, and the attachment of neuron and glial cells, neurite extension, and dendritic arborizations were examined. We further monitored the intracellular mass transport of vesicles within the cell bodies of the neurons and through the neurites using a form of quantitative phase imaging called spatial light interference microscopy (SLIM). These results will be broadly useful to improve efforts to understand the developmental and physiological processes of neural tissues for the treatment of neural injuries and disorders.

2. Experimental method

2.1. Production and purification of recombinant, soluble N-cadherin extracellular domains

Soluble, recombinant N-cadherin ectodomains with C-terminal Fc tags (N-cadherin-Fc) were stably expressed in human embryonic kidney cells (HEK293, American Type Culture Collection), as previously described [39,40]. Cells were cultured in Dulbecco's Modified Eagle Medium (DMEM) containing 10% (v/v) fetal bovine serum (FBS) and 0.4 mg/mL G418 (Sigma Aldrich) as a selection marker. The cell culture supernatant containing the recombinant N-cadherin protein was collected every two to three days. The supernatant was later filtered and purified using a protein-A affinity column (Bio-Rad) and gel filtration chromatography (HiPrep

Please cite this article as: E. C. Qin, M. E. Kandel, E. Liamas et al., Graphene oxide substrates with N-cadherin stimulates neuronal growth and intracellular transport, Acta Biomaterialia, https://doi.org/10.1016/j.actbio.2019.04.005

16/60 Sephacryl S-200 HR, Sigma-Aldrich) using the AKTA pure protein purification system. Protein purity was assessed using sodium dodecyl sulfate polyacrylamide gel electrophoresis (SDS-PAGE).

2.2. Preparation of graphene oxide (GO) and reduced graphene oxide (rGO) suspension

Dry graphene oxide platelets (GO), with a diameter of 0.2–2, μm and a thickness of 1.1 ± 0.2 nm, was purchased from the manufacturer (Graphene Supermarket, Product Number: SKU-GO-005). Reduced graphene oxide (rGO), prepared by thermal exfoliation and hydrogen reduction of graphene oxide with a diameter of 0.4–0.5 μm and a thickness between 0.6 and 1.2 nm, was purchased from the manufacturer (ACS Materials, Product Number: GN1P0005). GO was suspended in 70% ethanol and rGO was suspended in 70% ethanol and 0.5% sodium dodecyl sulfate to a final concentration of 1 mg/mL and sonicated for 1 h before use to ensure the GO and rGO are in single layers and separated from each other.

2.3. Surface modification of glass with GO/rGO and N-cadherin

Glass coverslips were plasma treated with air for 1 min to render the surface hydrophilic. Then, 15 μL of either GO or rGO flakes in suspension at a concentration of 1.0 mg/mL were spin coated onto the glass. The coated glass substrates were then incubated at 55 °C for 10 min, to evaporate the ethanol and water from the glass substrate, and to facilitate the uniform distribution of GO and rGO onto the glass surface. As the drying temperature was lower than the temperature used to reduce GO, the drying process did not result in significant reduction of GO and rGO (Fig. A1) [41]. The resulting coated glass substrates were incubated with 50 μg/mL N-cadherin-Fc in phosphate-buffered saline with calcium (cPBS) for 1 h at room temperature. Six conditions were tested as shown in Table 1.

2.4. FTIR and XPS characterization of GO/rGO flakes

The compositions of GO and rGO were determined using Fourier transform infrared (FT-IR) and X-ray photoelectron spectroscopy (XPS). For FT-IR, samples were prepared by pressing ~1 wt% GO/rGO flakes that were thermally treated with the conditions described in Section 2.3 together with potassium bromide (KBr, Sigma Aldrich) to form a transparent pellet. The spectra of the pellets were recorded using a Thermo-Nicolet Nexus 670 at a spectral range between 1000 and 4000 cm^{-1}. The resulting spectra was the result of 64 scans obtained at a resolution of 4 cm^{-1}, and the baseline for the spectra was corrected in Origin using the 2nd derivative method and connected using the spline interpolation method. The Asymmetric Least Squares Smoothing Baseline Method was used to smooth the spectra. For XPS, the samples were prepared by depositing a thick layer of GO/rGO onto a glass via repeated drop drying, and thermal treatment with the conditions described in Section 2.3. XPS measurements were acquired using a Kratos Axis ULTRA with a monochromated Al-K_α X-ray source ($h\nu$ = 1486.61 eV). The atomic ratios of carbon to oxygen were calculated from the survey spectra by considering the integrated areas of their respective peak positions (294.5 and 533.0 eV). The deconvolution of the carbon spectra was performed using the CasaXPS software.

2.5. Spatial distribution and characterization of GO/rGO spin-coated onto glass using Raman spectroscopy

The Raman spectra of the glass substrates coated with GO/rGO were acquired in air at ambient conditions with a Nanophoton Raman-11 Laser Microscope. The spectra were recorded with a 532-nm laser between 1000 and 3000 cm^{-1}. For Raman XY mapping, a surface area of 140 × 140 μm^2 was recorded using a 20× objective lens (numerical aperture NA = 0.45). The laser beam was focused on each point for a 0.01 s exposure time and averaged two times per point, and the samples were measured at 35 × 35 pixels with a resolution of 4.1 μm. The data was further processed using a Raman image processing software (Raman Viewer; Nanophoton Corporation, Japan) to generate the average Raman spectra with baseline correction and normalization and to plot the surface maps of GO/rGO. The Raman maps show the total intensity of D-band (1320–1370 cm^{-1}) and G-band (1550–1610 cm^{-1}) to the intensity of the second-order optical phonon peak (850–1050 cm^{-1}) of the glass substrate in the Raman spectrum.

2.6. Surface energy of glass modified with GO/rGO

The contact angles of water and methylene iodide (Sigma Aldrich) were recorded using the sessile drop method with a Rame-Hart Contact Angel Goniometer. The DROPimage Standard software was used to calculate the surface energy of the various substrates. The surface energy was based on a two component model for solid surface energy developed by Owens and Wendt, as described in the equation below (1):[42]

$$\frac{\sigma_L(cos\theta+1)}{2(\sigma_L{}^D)^{1/2}} = (\sigma_S{}^P)^{1/2}\left(\frac{\sigma_L{}^P}{\sigma_L{}^D}\right)^{1/2} + (\sigma_S{}^D)^{1/2} \quad (1)$$

where: σ_L = overall surface tension of the liquid, σ_L^D = dispersive component of the surface tension of the liquid, σ_L^P = polar component of the surface tension of the liquid, σ_S = overall surface energy of the solid, σ_S^D = dispersive component of the surface energy of the solid, σ_S^P = polar component of the surface energy of the solid, σ_{SL} = the interfacial tension between the solid and the liquid, and θ = the contact angle between the liquid and the solid. For water, σ_L = 72.8 erg/cm^2, σ_L^D = 21.8 erg/cm^2, and σ_L^P = 51.0 erg/cm^2. For methylene iodide, σ_L = 50.8 erg/cm^2, σ_L^D = 48.5 erg/cm^2, and σ_L^P = 1.3 erg/cm^2. The total surface energy of the surface is the sum of the slope, $(\sigma_s^P)^{1/2}$, and the intercept, $(\sigma_s^D)^{1/2}$.

2.7. Circular dichroism analysis of N-cadherin secondary structure

To prepare the samples, 0.28 μg/mL recombinant N-cadherin-Fc solution was mixed with 0.20 mg/mL GO or rGO suspension for one hour at room temperature. All samples were prepared in cPBS. Circular dichroism (CD) measurements of unbound N-cadherin and N-cadherin associated with GO and rGO flakes were conducted using

Table 1
Experimental conditions.

Samples	Condition 1	Condition 2	Condition 3	Condition 4	Condition 5	Condition 6
GO	–	+	–	–	+	–
rGO	–	–	+	–	–	+
N-cadherin-Fc	–	–	–	+	+	+

Please cite this article as: E. C. Qin, M. E. Kandel, E. Liamas et al., Graphene oxide substrates with N-cadherin stimulates neuronal growth and intracellular transport, Acta Biomaterialia, https://doi.org/10.1016/j.actbio.2019.04.005

the Jasco 715 spectropolarimeter. A quartz cell with an optical path length of 1 mm was used. The scanning speed was set at 50 nm/min, and a wavelength range was examined between 200 and 250 nm.

2.8. Enzyme-linked immunosorbent assay (ELISA) to determine amount of adsorbed N-cadherin

A mass balance approach was used to quantify the amount of N-cadherin immobilized on the coated and uncoated glass substrate. After incubation with the glass substrates, the unbound N-cadherin was collected and added to a polystyrene 96-well plate. After incubation for 1 h at 37 °C, the plate was washed and then incubated with 2% bovine serum albumin (BSA) in cPBS for 1 h at 37 °C to block nonspecific interactions. Then, the wells were incubated with N-cadherin rabbit polyclonal antibody (1:600, ProteinTech) overnight at 4 °C. Horse radish peroxidase (HRP)-conjugated anti-rabbit IgG (1:10,000, Sigma Aldrich) was added to each well and incubated at room temperature for one hour. Between each step, the wells were washed extensively with cPBS. A 3,3′,5,5′-tetramethylbenzidine (TMB) ELISA substrate kit (ThermoFisher) was used as a chromogenic substrate for HRP. After incubation for 20 min with the TMB and peroxide solution from the kit, the absorbance of each well was measured at 370 nm with a microplate reader (Tecan Infinite 200 PRO). A calibration curve was conducted with known amounts of N-cadherin and their corresponding absorbance to determine the surface density of N-cadherin immobilized on the substrate.

2.9. Atomic force microscopy imaging and adhesion force measurement

Topographic images and force–displacement curves were acquired using a Multimode Nanoscope III atomic force microscope (AFM) equipped with Nanoscope III controller (Veeco, CA). Silicon nitride AFM cantilevers, with a nominal spring constant of 0.27 N/m, (nominal spring constant 0.27 N/m) were purchased from BudgetSensors (Sofia, Bulgaria). AFM was operated in intermittent contact mode for imaging on substrates with and without N-cadherin. One hundred force curves were collected with unmodified AFM tips over a $10 \times 10\ \mu m^2$ region on either GO or RGO cluster with or without N-cadherin, using the aid of the system integrated optical microscope. This process was repeated over three different locations on the substrates, in order to acquire a total of 300 force curves for each sample examined. The applied load and tip retraction velocity were kept at 4 nN and 2 μm/s respectively for the force measurements. Surface adhesion values were quantified by registering the force required to separate the AFM tip from surface, and analyzed using Matlab scripts (developed by Carpick's group at the University of Pennsylvania). All experiments were performed in cPBS at room temperature.

2.10. Primary hippocampal neuron culture

All experimental procedures were performed with protocols approved by the Institutional Animal Care and Use Committee, University of Illinois at Urbana-Champaign, and in compliance with the principles and procedures outlined in the National Institutes of Health Guide for the Care and Use of Laboratory Animals. Hippocampal neurons were obtained from neonatal (P1-P2) Long-Evans BluGill rat brains, as previously described. After isolation, the hippocampi were placed in Hibernate-A (Brain Bits, Springfield, IL) on ice, and then treated with 18 U/mL papain (Sigma Aldrich) in Hibernate-A for 30 min at 37 °C. Following enzymatic digestion, the hippocampi were rinsed with Hibernate-A, and mechanically dissociated through trituration using a fire-polished Pasteur pipette. The dissociated cells were centrifuged and re-suspended in standard maintenance media containing Neurobasal media (Gibco), supplemented with 0.5 mM GlutaMAX (Gibco), serum-free neural media supplement (GS21, Sigma Aldrich), 100 U/mL penicillin and 0.1 mg/mL streptomycin.

Prior to cell culture, the coated and uncoated glass substrates were incubated with complete culture medium for 15 min at 37 °C. Primary hippocampal neurons were seeded onto the different glass substrates prepared as summarized in Table 1. For low-density cell experiments, the cells were seeded at a density of 150,000 cells/cm^2, and cultured at 37 °C in the presence of 5% CO_2. For high density, long-term cell experiments, the cells were seeded at a density of 375,000 cells/cm^2, and the osmolality of the medium was adjusted to 275 mOsm with sodium chloride. For the low and high cell density experiments, half of the medium was removed and replaced with fresh maintenance medium every three days.

2.11. Immunofluorescence imaging and neuronal analysis

After 4 and 10 days of culture, the cells on the coated and uncoated glass substrates were fixed with acetone:methanol (1:1) for 20 min at −20 °C and then were blocked with 2% BSA for 30 min. The cultures were then incubated with rabbit polyclonal anti-microtubule associated protein 2 (MAP2) (1:500, Abcam) and mouse anti-glial fibrillary acid protein (GFAP) (1:250, BD Biosciences) overnight at 4 °C. Afterwards, the cells were incubated with fluorescently labeled goat anti-rabbit (H + L) cross-adsorbed secondary antibody Alexa Fluor 488 (1:25, ThermoFisher) and goat anti-mouse IgG (H + L) Alexa Fluor 555 (1:250, Cell Signaling Technology) for 60 min at room temperature. Finally, the cell nuclei were stained with DAPI (10 μg/mL, Invitrogen) for 8 min at room temperature. Between steps, the coated and uncoated glass substrates were rinsed with PBS. The immunofluorescence imaging was obtained using a confocal microscope (Zeiss LSM 700). Afterwards, ImageJ was used to quantify the total number of cells stained for GFAP and MAP2, the number of primary and terminal neurites, and the length of the neurites. Due to clustering of cells present on the glass substrate, several assumptions are made to quantify the neuronal behavior on the glass substrate for the higher density cultures. First, to estimate the number of dendrites, the width of the dendrites was divided by the average width of the individual dendrites, measured from the dendrites on neurons cultured on the N-cadherin coated GO and rGO substrates. Second, to estimate the number of cells, only cells that had direct contact with the substrate was counted. Third, morphological conditions was used to classify neurons from glial cells.

2.12. Label-free intracellular transport with quantitative phase imaging

Spatial Light Interference Microscopy (SLIM), a technique that measures the optical path length shifts in the phase contrast geometry, was used to examine the intracellular mass transport in the neuronal cell body and neurites. Images were acquired with a SLIM system (CellVista SLIM Pro, Phi optics, Inc.) attached to a Zeiss Z1 microscope, as described previously [33]. The cells were seeded at 250,000 cells cells/cm^2 in maintenance medium. After 22 h in culture, the neurons were continuously monitored (in "bursts") for 12 min at each field-of-view with a separation of 5.5-hour time intervals between bursts for a total of approximately 40 h. During imaging, the cells were kept at 37 °C and in a 5% CO_2 atmosphere with an incubator and heated stage insert (Zeiss). To characterize mass transport phenomena, the mean spread of advection velocities was examined using dispersion-relation phase spectroscopy

Please cite this article as: E. C. Qin, M. E. Kandel, E. Liamas et al., Graphene oxide substrates with N-cadherin stimulates neuronal growth and intracellular transport, Acta Biomaterialia, https://doi.org/10.1016/j.actbio.2019.04.005

(DPS), a method that uses time-resolved quantitative phase imaging to analyze intracellular transport [27,30]. The phase map time-sequence was manually annotated into neurites and bodies using ImageJ to yield a single advection spread coefficient [32].

2.13. Statistical analysis

All *in vitro* experiments were conducted with at least two independent cell experiments and with at least four different samples per group. All results represented mean ± standard error of mean, unless otherwise noted. For *in vitro* experiments, a one-analysis of variance (ANOVA) followed by Tukey-HSD post-hoc tests were performed on all data sets. For SLIM experiments, a Wilcoxon rank-sum test was used to compare between groups, and the data was reported as a box-and-whisker plot, where the whiskers show the minimum and maximum, and the box shows the 25th, 50th, and 75th percentiles.

3. Results

3.1. Characterization of GO and rGO flakes

Fourier-transform infrared (FT-IR) spectra of the functional groups of GO and rGO flakes are shown in Fig. 1a. GO flakes have peaks at 3400, 1730, 1412, 1225, and 1047 cm^{-1}, which correspond to the O—H, C═O, C═C, C—O—C, and C—O groups, respectively. In contrast, rGO flakes only exhibit some of the oxygen containing functional groups (C═O, C═C, and C—O—C). This result was re-confirmed with X-ray photoelectron spectroscopy (XPS). XPS elemental analysis shows that the carbon to oxygen atom ratio of GO is 0.46, while that of rGO is 2.14, due to the reduction of the epoxides and hydroxyl groups (Fig. 1b). Both GO and rGO have peaks at 284.6 eV, which corresponds to the emission from the sp^2-hybridized carbons. However, GO has another higher binding energy peak at 286.7 eV, which is assigned to the hydroxyl group, as well as an additional peak at 289.4 eV, which corresponds to the carboxylic acid group (Fig. 1c). rGO showed smaller peaks corresponding to hydroxyl and carboxylic acid groups than GO (Fig. 1d).

3.2. Characterization of glass substrates coated with GO and rGO flakes

GO and rGO flakes were spin-coated onto plasma-treated glass substrates. Raman spectroscopy of glass coated with GO or with rGO flakes revealed two broad peaks: a D-band at ~1,360 cm^{-1} and a G-band ~1,600 cm^{-1}. The D-band represents the out-of-plane vibrations of sp^2 carbon due to the presence of structural defects, and the G-band represents the in-plane vibrations of sp^2 carbon from a 532-nm excitation laser. The additional oxygen-containing functional groups on GO disrupted the in-plane sp^2 configuration and resulted in a higher relative peak intensity ratio of the D- to the G-band (~1.06) than rGO flakes (~0.72). The ratio of the G-band at ~1,360 cm^{-1} to the 2D band at ~1,600 cm^{-1} was 0.21 for glass coated with GO and 0.17 for glass coated with rGO. This result states that the GO and rGO are single-layered [43]. Raman spectroscopy mapping and confocal images of the total intensity of D-band (1320–1370 cm^{-1}) and G-band (1550–1610 cm^{-1}) confirmed that GO and rGO flakes were evenly distributed across the surface (Fig. 2b). Confocal images showed that the surface coverage of GO and rGO to the glass substrates were around ~40%. There was no significant difference between the surface coverage of GO and rGO.

Water contact angle measurements showed that glass substrates coated with GO and rGO flakes were more hydrophobic than uncoated glass substrates, as noted by the increased advancing water contact angles (Fig. 2c). As expected, the glass substrate coated with rGO flakes was slightly more hydrophobic than the glass substrate coated with GO flakes. The contact angle of water was 31 ± 3° for GO, and 38 ± 3° for rGO. For glass, the contact angle of water was only 19 ± 2°. The total surface energy of glass substrates coated with GO or rGO flakes was calculated based on the

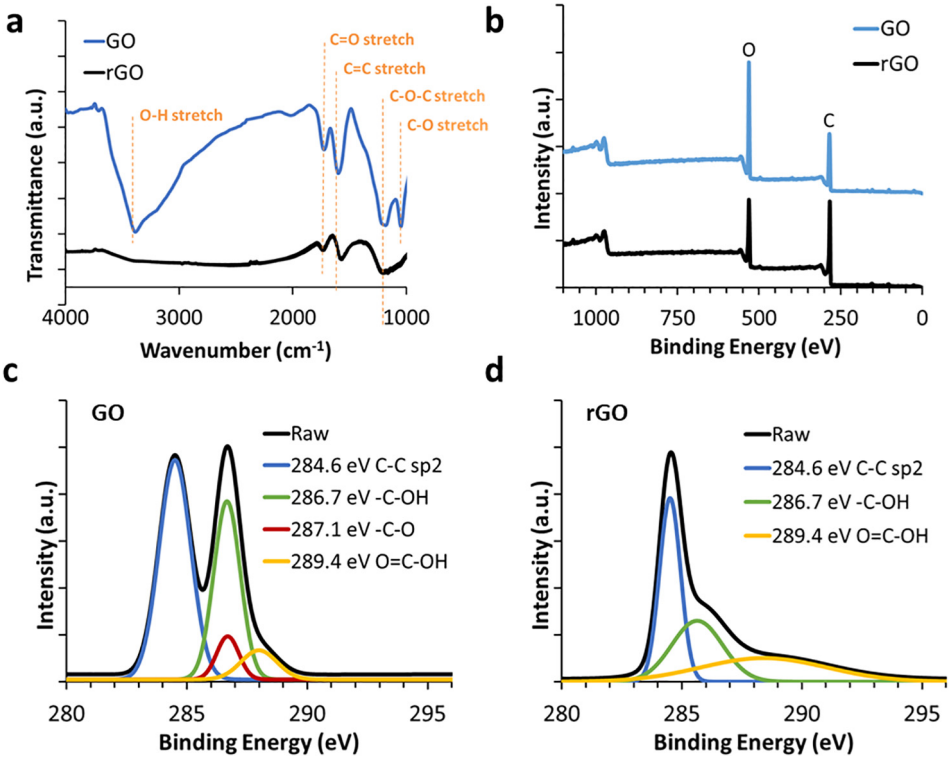

Fig. 1. Characterization of GO/rGO flakes. (a) FT-IR spectra of GO/rGO flakes. (b) XPS elemental analysis. Deconvolution of the C1s XPS spectra of (c) GO and (d) rGO.

Please cite this article as: E. C. Qin, M. E. Kandel, E. Liamas et al., Graphene oxide substrates with N-cadherin stimulates neuronal growth and intracellular transport, Acta Biomaterialia, https://doi.org/10.1016/j.actbio.2019.04.005

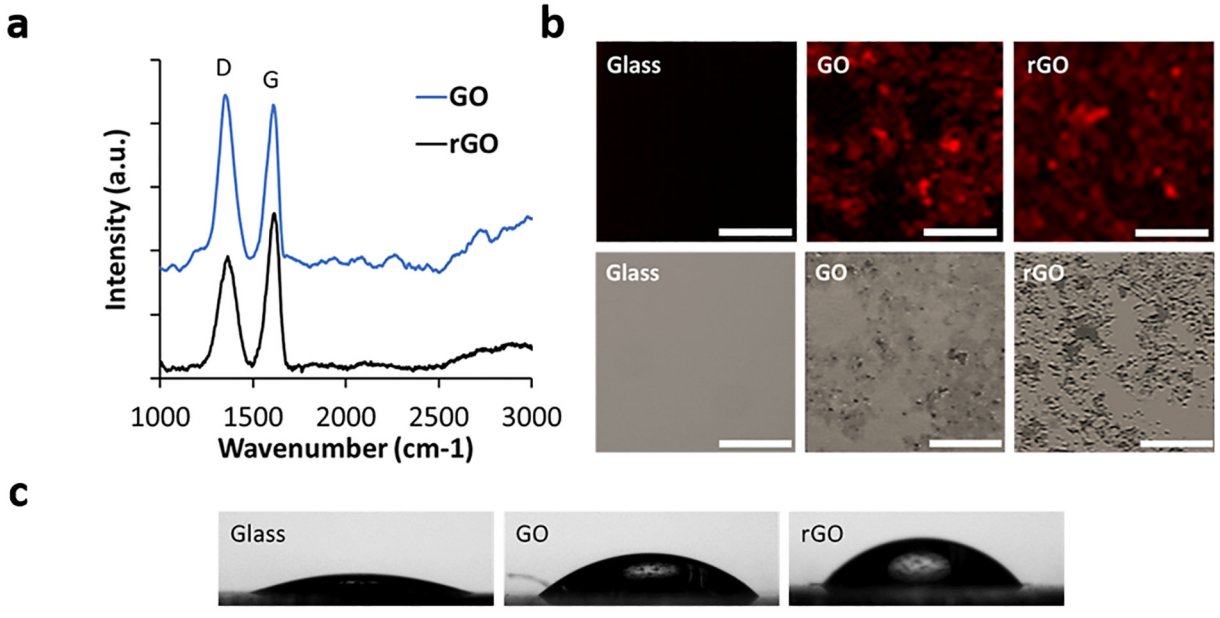

d

Sample	Contact Angle of Water (°)	Polar Surface Energy (mN/m)	Dispersive Surface Energy (mN/m)	Total Surface Energy (mN/m)
Glass	19 ± 2	34 ± 1	40 ± 1	74 ± 1
GO coated glass	31 ± 3	34 ± 1	32 ± 1	65 ± 2
rGO coated glass	38 ± 3	22 ± 2	45 ± 2	68 ± 2

Fig. 2. Surface analysis of GO/rGO coated substrates. (a) Raman spectroscopy of GO and rGO. (b) *1st row:* Representative intensity mapping of the total intensity of the D-(1320–1370 cm^{-1}) and G-band (1550–1610 cm^{-1}). *2nd row:* Corresponding phase contrast confocal images of substrates. Scale bar represents 50 μm. (c) Images of water droplets on uncoated, GO and rGO-coated glass. (d) Table of the contact angle and surface energy of the substrates. The values represent the mean ± the standard error of the mean (n = 4).

two-component model developed by Owens and Wendt to be around 65 ± 2 and 68 ± 2 mN/m, respectively [42]. This value was around 10 mN/m lower than that of the uncoated glass substrate (Fig. 2d).

3.3. Physisorption of N-cadherin onto GO/rGO-coated glass substrates

Recombinant N-cadherin molecules were physisorbed onto the surface of un-, GO-, or rGO-coated glass by exposing the substrates to a solution of 50 μg/mL N-cadherin-Fc (Fig. 3a). AFM images acquired in PBS containing calcium showed that N-cadherin adhered to all three substrates (Fig. 3b, Fig. A2), and the adsorbed protein was approximately 2–3 nm in height with an average diameter of 15 nm (Fig. A3). In comparison with prior electron microscopy images of N-cadherin on mica [44], the images presented here suggest that N-cadherin adsorbs as aggregates or as 'collapsed' globules.

AFM-based force spectroscopy was used to quantify the surface adhesion between an uncoated AFM tip and the N-cadherin layer on the uncoated, GO, and rGO-coated glass. The adhesion is defined as the force required to separate the AFM tip from the solid surface, with or without the N-cadherin (Fig. A4). It was found that the GO- and rGO-coated glass substrates had greater mean adhesion strength of N-cadherin than uncoated glass substrates. The surface adhesion of uncoated glass is approximately 0.57 ± 0.04 nN, as measured by AFM. In contrast, the mean adhesion strength of N-cadherin to the GO- or rGO-coated glass substrates was approximately ten times higher than the uncoated glass substrate (Fig. 3c). While the mean values do not demonstrate a significant difference in adhesion strength, the force histogram distribution were much broader for the N-cadherin layer on GO- and rGO-coated glass. In addition, the maximum adhesion, determined by the peak of the histogram, appeared to shift to higher values on the rGO-coated glass. rGO (~3.5 nN) had a maximum surface adhesion between the N-cadherin and AFM tip, compared to uncoated glass (~1 nN) and GO (~2 nN). Control studies of the adhesion between AFM and the uncoated, GO-, and rGO-coated glass without N-cadherin revealed a significantly lower adhesion over all samples (Fig. A5). This result confirmed that the adhesion force was dependent on the interaction between the N-cadherin layer and AFM tip, which was influenced by the underlying substrate. Importantly, these measurements did not quantify the strengths of individual cadherin bonds [25,45], but rather semi-quantitatively compared the relative adhesion of the AFM tip to the different substrates. This was apparent from the high values of the reported adhesion (nN) relative to the piconewton forces to rupture individual cadherin bonds [25]. The force-extension curves also indicated multiple unbinding events over retraction distances of more than 150 nm.

We separately examined whether GO and rGO also increased the total number of N-cadherin physiosorbed to the various substrates using an enzyme-linked immunosorbent assay (ELISA) (Fig. 3d). Interestingly, GO and rGO did not increase the total density of N-cadherin bound to the glass substrate, compared to the N-cadherin adhered to the uncoated glass. GO and rGO-coated glass resulted in slightly higher amounts of physisorbed N-cadherin

Please cite this article as: E. C. Qin, M. E. Kandel, E. Liamas et al., Graphene oxide substrates with N-cadherin stimulates neuronal growth and intracellular transport, Acta Biomaterialia, https://doi.org/10.1016/j.actbio.2019.04.005

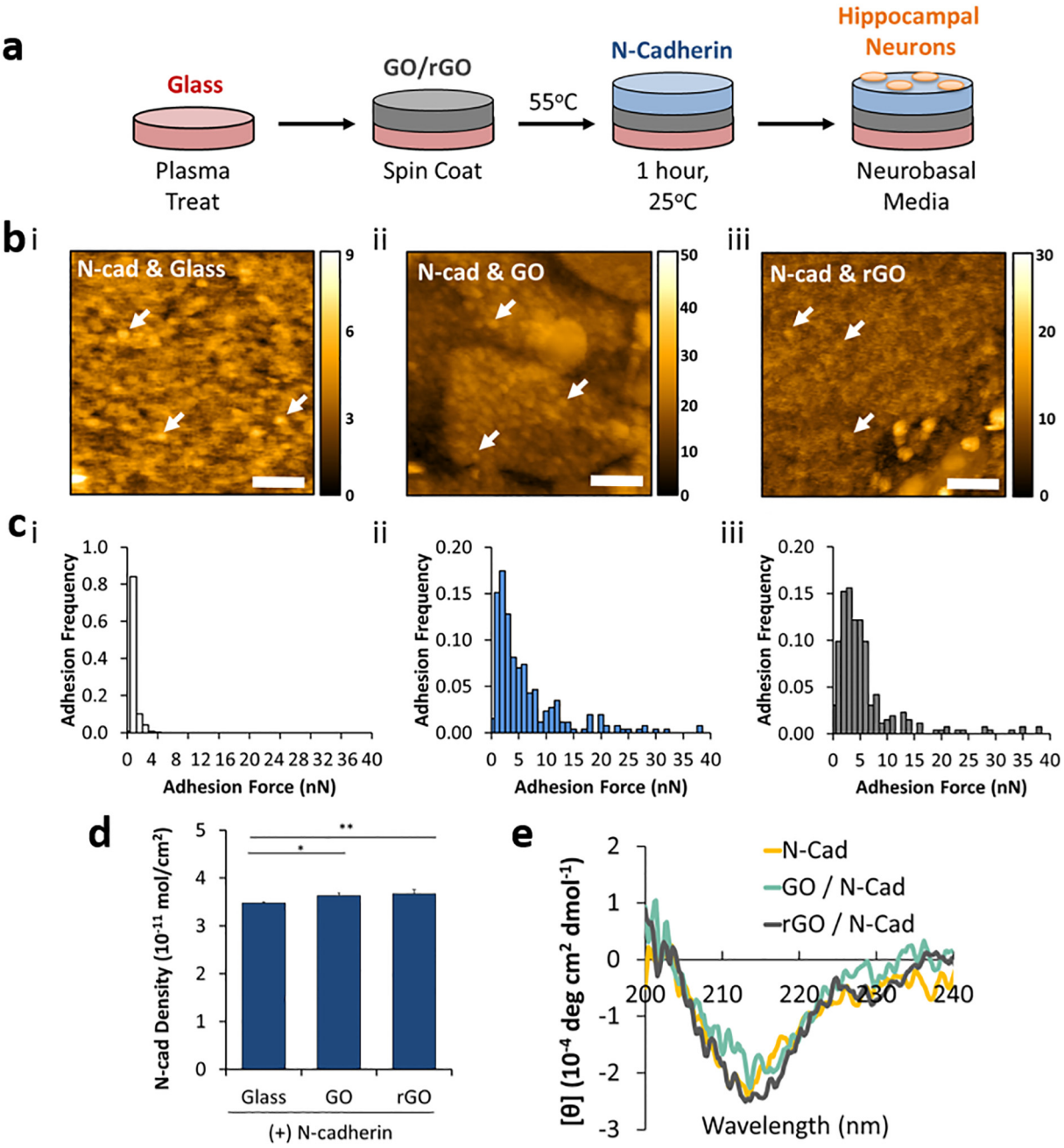

Fig. 3. Immobilization of N-cadherin onto GO/rGO-coated glass surfaces. (a) Scheme that depicts the procedure to immobilize N-cadherin on the GO/rGO-coated substrates. (b) AFM images N-cadherin adhered onto (i) uncoated glass, (ii) GO-coated glass, and (iii) rGO-coated glass. AFM experiments were performed in liquid, and the arrows represent areas where N-cadherin molecules are bound. The scale bar represents 100 nm. (c) Adhesion force histograms obtained by force-distance curves for N-cadherin adhered on (i) the uncoated glass, (ii) GO-coated glass, and (iii) rGO-coated glass. (d) Average density of adsorbed N-cadherin on the various substrates (n = 3). * represents a p-value < 0.05 and ** represents a p value < 0.01 by a one-way ANOVA. (e) Circular dichroism spectra of either soluble N-cadherin or N-cadherin physiosorbed to GO or rGO flakes.

(0.36 ± 0.06 and 0.37 ± 0.08 pmol/cm^2, respectively) than uncoated glass (0.34 ± 0.02 pmol/cm^2). In addition, circular dichroism spectroscopy confirmed that N-cadherin mixed with the GO or rGO flakes in solution retained its original beta-sheet confirmation, with a negative band at 212 nm (Fig. 3e).

3.4. Enhanced N-cadherin adhesive function on GO/rGO-coated glass substrates promotes neuronal cell adhesion and dendritic arborization

Primary rat hippocampal neurons were cultured on the different substrates, and the morphologies of neurons seeded on the different substrates were evaluated by staining neurons and glial cells with microtubule associated protein 2 (MAP2) and glial fibrillary acidic protein (GFAP), respectively, after four days *in vitro*. To investigate the neuronal morphologies, the cells were seeded at an initial low density of 150,000 cells/cm^2. N-cadherin adsorbed on GO-coated glass substrates (N-cadherin-GO-glass) or N-cadherin adsorbed on rGO-coated glass substrates (N-cadherin-rGO-glass) increased the percentage of MAP2-positive neurons relative to neurons on glass. In contrast, N-cadherin adsorbed on the uncoated glass (N-cadherin-glass) did not increase the number of MAP2-positive neurons, compared to cells on the uncoated glass substrate (Fig. 4a & b; Fig. A6). All conditions resulted in minimal adhesion of glial cells (~1–4%), stained with GFAP. Treatment with

Please cite this article as: E. C. Qin, M. E. Kandel, E. Liamas et al., Graphene oxide substrates with N-cadherin stimulates neuronal growth and intracellular transport, Acta Biomaterialia, https://doi.org/10.1016/j.actbio.2019.04.005

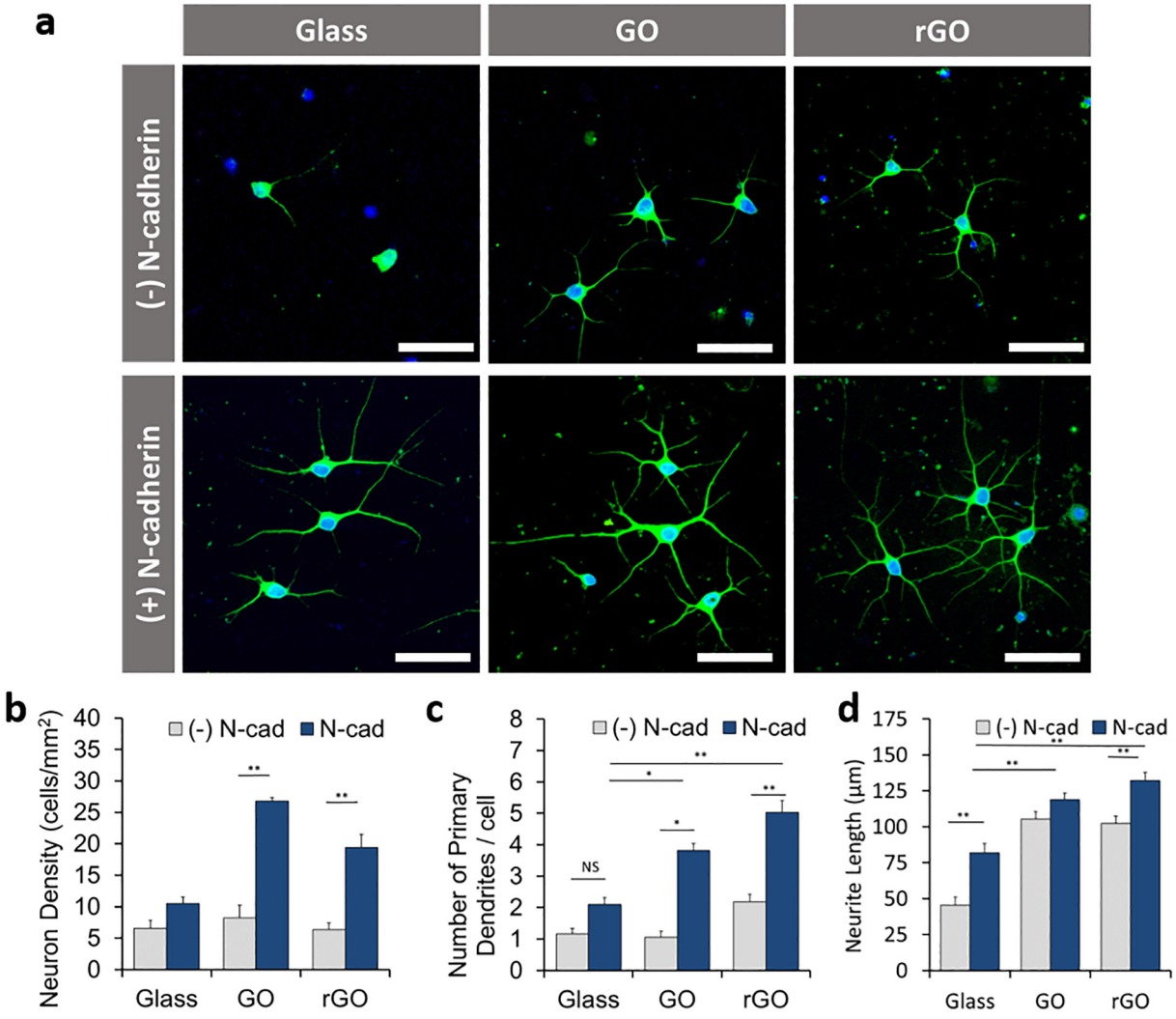

Fig. 4. Hippocampal neurons cultured on substrates modified with physisorbed N-cadherin on GO- or rGO-coated glass. Cells were seeded at a density of 150,000 cells/cm^2 and imaged at 4 days *in vitro*. (a) Representative confocal images of hippocampal neurons on uncoated, GO-, and rGO-coated substrates immobilized with and without N-cadherin. Scale bar represents 50 μm. Green represents MAP2 and blue represents DAPI. Quantification of (b) density of neurons stained for MAP2 (n = 4 per group), (c) number of primary dendrites per cell, (n > 30 cells per group) and (d) average neurite length (n > 50 neurites per group). In all figures, * represents a p value < 0.05 and ** represents a p-value < 0.01 as determined by a one-way ANOVA with Tukey's post-hoc. The bars represent the mean values ± the standard error of mean. (For interpretation of the references to color in this figure legend, the reader is referred to the web version of this article.)

N-cadherin function-blocking antibody prevented cell attachment to the glass substrates with physisorbed recombinant N-cadherin (Fig. A7), which confirmed the binding specificity of the adhesive N-cadherin ligand.

In addition, N-cadherin-GO-glass and N-cadherin-rGO-glass increased the number of primary dendrites per cell by 2.5 and 4-fold, respectively, compared to GO- and rGO-coated glass substrates without N-cadherin (Fig. 4a & c, Fig. A8). Furthermore, on N-cadherin-rGO-glass, the mean lengths of the neurites and the number of primary dendrites extended from the neuron were greater than on the uncoated glass (Fig. 4a & d). In the absence of N-cadherin, the neurite length was only slightly higher on GO- or rGO-coated glass compared with cells on the uncoated glass. Interestingly, none of the coatings affected dendritic arborization.

The effects of N-cadherin and GO/rGO flakes on neurons were further observed when neurons were plated at sub-confluent densities for long-term culture. As it was difficult to maintain cultures of primary neurons at low cell densities due to the lack of trophic support from adjacent neurons and glia [46], the neurons were seeded at a higher density of 375,000 cells/cm^2. After 3 days *in vitro* on N-cadherin-glass, the neurons self-aggregated to form clusters (Fig. A9). The clusters showed limited dendritic arborization by 9 days *in vitro* (Fig. 5a; Fig. A9). In contrast, neurons cultured on the N-cadherin-GO-glass or on N-cadherin-rGO-glass did not form clusters. Instead, the neurons were homogenously distributed across the substrates, and formed extensively interconnected neural networks. Uncoated and coated glass substrates without physisorbed N-cadherin did not support long-term cultures past 4 days *in vitro* (Fig. A10).

Because the neurons clustered on N-cadherin-glass, it was difficult to determine the total number of cells adhered to the surface, the cell types, and the number of dendritic extensions per neuron. For instance, the cluster prevented proper labeling of neuron and glial cells within the clusters. In addition, multiple neurites were grouped together, which made discerning the source of the neurites from individual neuronal cell bodies impossible. By contrast, valuable information could be perceived from the neurons that were evenly distributed over the substrates. The density of neurons that adhered to the N-cadherin-GO-glass was higher than the number of neurons adhered on N-cadherin-rGO-glass glass

Please cite this article as: E. C. Qin, M. E. Kandel, E. Liamas et al., Graphene oxide substrates with N-cadherin stimulates neuronal growth and intracellular transport, Acta Biomaterialia, https://doi.org/10.1016/j.actbio.2019.04.005

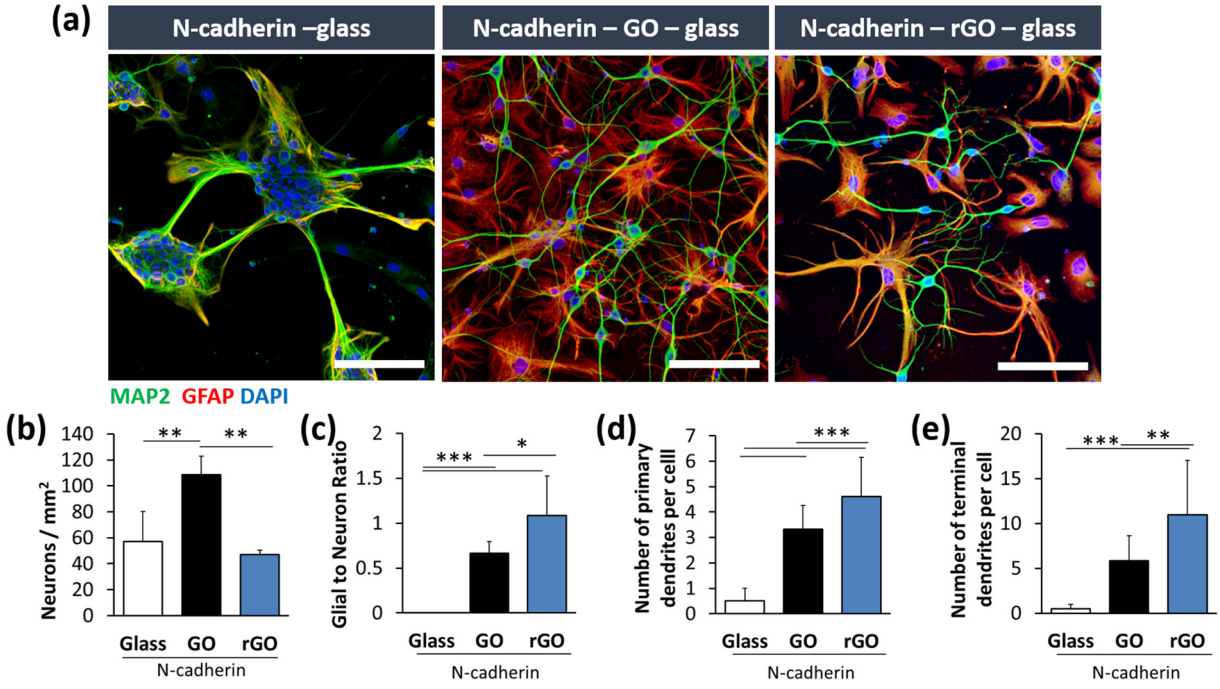

Fig. 5. High density neuronal cultures on substrates coated with GO/rGO and immobilized with N-cadherin. Cells were seeded at a density of 375,000 cells/cm^2 and imaged at 10 days *in vitro*. (a) Representative confocal images of hippocampal neurons on uncoated, GO-, and rGO- coated substrates immobilized with and without N-cadherin. Scale bars represent 100 μm. The green color represents, the red color represents GFAP, and the blue color represents DAPI. Quantification of the (b) neuronal density (n = 4 per group), (c) neuron to glial ratio (n = 4 per group), (d) number of primary dendrites per cell (n > 30 cells per group), and (e) the total number of terminal dendrites per cell (n > 30 cells per group). In all figures, * represents a p-value < 0.05, ** represents a p-value < 0.01, and *** represents a p-value < 0.001 as determined by a one-way ANOVA with Tukey's post-hoc. The bars represent the mean values ± the standard error of mean. (For interpretation of the references to color in this figure legend, the reader is referred to the web version of this article.)

(Fig. 5b, Fig. A11). N-cadherin-GO-glass facilitated the adhesion of glial cells marked with GFAP compared to the two other conditions, which resulted in a higher neuron to glia ratio on the N-cadherin-rGO-glass than on the N-cadherin-GO-glass (Fig. 5a & c, Fig. A12). In addition, neurons cultured on the N-cadherin-rGO-glass displayed greater primary and terminal arborization than those grown on N-cadherin-GO-glass (Fig. 5a, d & e, Fig. A8). The arborization of primary dendrites originating from the cell body of the neurons was 3 ± 1 primary dendrites per cell on N-cadherin-GO-glass and 5 ± 2 primary dendrites per cell on N-cadherin-rGO-glass. The total number of terminal neurites was also two times higher on N-cadherin-rGO-glass (6 ± 3 terminal dendrites per cell) than that on N-cadherin-GO-glass (11 ± 6 terminal dendrites per cell).

3.5. N-cadherin modulates intracellular mass transport through interconnected neurons

To determine how the different substrates affected neuronal functions, we quantified the intracellular vesicular mass transport throughout the neurites and cell body using a non-invasive and label-free quantitative phase imaging modality called spatial light interference microscopy (SLIM) [33].

Within the neuronal cell bodies, the intracellular mass transport was more active on substrates physiosorbed with N-cadherin than glass substrates without N-cadherin, as demonstrated by the higher mean advection velocity (Fig. 6a & 6b; Movies A1–A6). The mean advection velocities for neurons cultured on uncoated, GO- and rGO-glass were 1.6 ± 0.3, 1.8 ± 0.6, and 1.6 ± 0.4 μm/min, respectively. On the other hand, the mean velocities of N-cadherin-glass, N-cadherin-GO-glass, and N-cadherin-rGO-glass, were 2.0 ± 0.4, 2.0 ± 0.4, and 2.0 ± 0.4 μm/min, respectively. GO and rGO flakes alone did not significantly affect the advection velocity in the cell body, regardless of the presence of N-cadherin (Fig. 6b).

Within the neurites, there was increased intracellular mass transport in neurons grown on N-cadherin-GO-glass and N-cadherin-rGO-glass compared to N-cadherin-glass. Interestingly, in neurons cultured on N-cadherin-GO-glass or on N-cadherin-rGO-glass, the mean advection velocity in the neurites increased (0.2 ± 0.2 and 0.3 + 0.2 μm/min, respectively), in comparison to transport in cells on N-cadherin-glass (0.1 ± 0.1 μm/min) (Fig. 6c & 6d; Movies A7–A9). Representative images of the time required for intracellular vesicular transport from one end to the other end of the frame are shown in Fig. 6c. Compared to the mean advection velocity in the cell body, the mean advection velocity in the neurites was 5–10 times slower. Neurons grown on glass without N-cadherin did not extend sufficient neurites for analyses of mass transport, due to shortened lengths and decreased dendritic arborizations. As a result, intracellular mass transport was only assessed in neurites on N-cadherin-glass.

4. Discussion

Results presented in this study show that soluble, recombinant N-cadherin extracellular domains retain greater adhesive function when physisorbed to GO or rGO coated glass, relative to N-cadherin directly adsorbed to uncoated glass. This resulted in greater neuron adhesion, arborization, and intracellular vesicle transport on N-cadherin-GO or N-cadherin-rGO-glass, relative to cells on N-cadherin-glass. Furthermore, AFM adhesion measurements confirmed greater N-cadherin-dependent tip-substrate adhesion to N-cadherin-GO or N-cadherin-rGO compared to N-cadherin-glass, at similar physisorbed protein densities.

We found that GO-glass and rGO-glass supported increased neuron adhesion and prevented cell clustering on N-cadherin mod-

Please cite this article as: E. C. Qin, M. E. Kandel, E. Liamas et al., Graphene oxide substrates with N-cadherin stimulates neuronal growth and intracellular transport, Acta Biomaterialia, https://doi.org/10.1016/j.actbio.2019.04.005

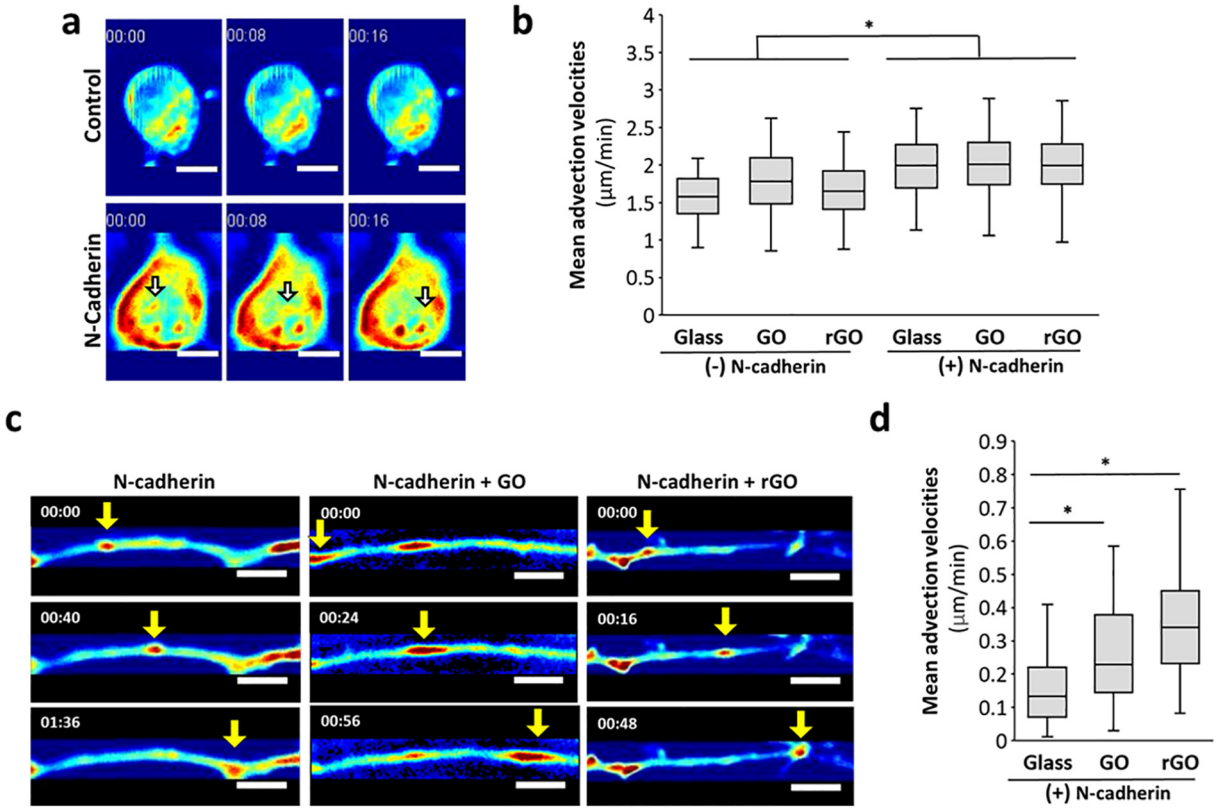

Fig. 6. SLIM-based quantitative imaging of mass transport of hippocampal neurons. (a) Representative images from SLIM of cell bodies on uncoated substrates immobilized with and without Ncadherin. The times are in minutes: seconds. Scale bar represents 5 μm. (b) Comparison of mean advection velocities of neuronal cell bodies (n > 30 cells per group). (c) Representative images from SLIM of neurites on uncoated and rGO-coated substrates immobilized with N-cadherin. The times are in minutes: seconds. Scale bar represents 5 μm. (d) Comparison of mean advection velocities in neurites (n > 45 neurites per group). The box plots show the 25th, 50th, and 75th percentiles, and the whiskers show the minimum and maximum. * represents a p-value < 0.05 as determined by the Wilcoxon rank-sum test.

ified substrates. Compared to cells adhered to N-cadherin-glass, N-cadherin-GO-glass and N-cadherin-rGO-glass resulted in increased neurite extension lengths and dendritic arborization. Also, hippocampal neurons adhered to the N-cadherin modified glass better than to glass without N-cadherin. This result indicates that neurons recognize and adhere to the recombinant N-cadherin molecules immobilized on the glass. More interestingly, neurons adhered to the N-cadherin-GO-glass or the N-cadherin-rGO-glass exhibited more active neurite extension and dendritic arborization than cells adhered to the N-cadherin-glass. This active neurite extension and dendritic arborization would allow for increased chances for synapse formation and communication between neighboring cells. In addition, despite the discontinuous, uncoated glass areas on N-cadherin-GO-glass and N-cadherin-rGO-glass, improvements in neuronal adhesion, neurite extension, and dendritic arborization can be observed. As the key difference between N-cadherin-glass and N-cadherin GO-glass or N-cadherin-rGO-glass is the presence of GO and rGO, respectively, the results suggest that these improvements are primarily due to GO and rGO.

In addition, we also found that GO-glass and rGO-glass supported glial cell adhesion, particularly with high initial seeding densities (375,000 cells/cm^2). Two-way communication between neurons and glial cells are extremely important for neuronal function. Glial cells, for instance, release neurotransmitters and other extracellular signaling molecules that affect synapse formation, synaptic transmission, and synaptic strength [47,48]. In this regard, glial cells are required for normal functioning of the nervous system. Previous studies have also shown that glial cells, which also express N-cadherin, binds preferentially to N-cadherin [49]. With lower density cultures (150,000 cells/cm^2), where glial cells were not present, we observed early neuronal death after four days of culture. By 10 days of culture, a majority of the neurons have died (~95%). In the presence of glial cells, the neurons interacted with the glial cells and the substrate. The neurons continued to grow and exhibit neurite arborizations after ten days of culture.

Numerous studies have shown that N-cadherin promotes neurite extensions [13,14]. It has been proposed that N-cadherin stimulates the neurite outgrowth through a "molecular clutch" mechanism, which involves a direct mechanical linkage between the N-cadherin/catenin complexes at the membrane and intracellular actin [8]. These results suggest that a critical density of functional N-cadherin bonds is required to stabilize adhesions and resist actin flow. The strength of single N-cadherin bonds is ~50 pN [45,50]. At the single molecule level, these individual weak bonds may not be sufficient to stabilize neuronal adhesion and support neurite extensions, but clusters of N-cadherin on beads used in optical trapping studies were capable of resisting actin flow, and N-cadherin adhesion to the cell surface stimulated neurite outgrowth [8]. Thus, increasing the population of active, physisorbed N-cadherin on the GO and rGO coated glass substrates, as suggested by AFM results presented here, would similarly increase the density of neuron-substrate bonds to a level sufficient to stabilize N-cadherin adhesions and support both neurite outgrowth and increased arborization. These results demonstrate increased dendritic outgrowth and arborization, neuronal adhesion, and intracellular transport on conditions with N-cadherin compared to the control (without N-cadherin). Therefore, we believe that there is a significant advantage to using N-cadherin for neuronal cultures, as without N-cadherin, we would not see the aforementioned effects. N-cadherin has been shown to pro-

Please cite this article as: E. C. Qin, M. E. Kandel, E. Liamas et al., Graphene oxide substrates with N-cadherin stimulates neuronal growth and intracellular transport, Acta Biomaterialia, https://doi.org/10.1016/j.actbio.2019.04.005

mote neuronal outgrowth more rapidly compared to non-adhesive polymers such as polylysine [14]; however, another paper reports that both N-cadherin and polylysine results high interconnected neuronal cultures [26]. As the exact mechanism for this behavior is complex, it is difficult to cross-compare the effects of N-cadherin to synthetic polymers.

Although the exact physical and chemical basis for the greater specific adhesion and amount of protein bound on the substrates is unclear, the results suggest that GO- and rGO-flakes bind Fc-tagged N-cadherin in a manner that both exposes the binding site and preserves the physiosorbed protein function. For instance, glass surfaces are negatively charged, so that the difference in retained N-cadherin activity could be due to the different effects of electrostatic versus van der Waals and non-polar interactions on the N-cadherin structure and activity. In contrast, the minimal difference in the adhesive function of N-cadherin-GO- and N-cadherin-rGO-glass implies that differences in local hydrogen bonding and electrostatic interactions between the GO/rGO flakes did not significantly alter the N-cadherin function. Our results indicated that the N-cadherin protein retains its original beta-sheet conformation when bound to both GO and rGO, unlike proteins such as insulin, which change conformation when bound to graphene derivatives [38].

Using SLIM, a highly sensitive form of quantitative phase imaging, we found that the presence of N-cadherin molecules on these substrates supported increased advection mass velocity in neurites, particularly when the protein was adsorbed onto the GO or rGO-coated glass. The ability of neurons to actively transport macromolecules and organelles is extremely important for forming physiologically functional neural networks. Proteins, soluble growth factors, and hormones are produced in the cell body, loaded in vesicles, and transported across the neurites [51]. As neurons grow and interact with neighboring proteins, neurons release intracellular molecules through exocytosis at the synaptic junction between cells. Defective transport due to protein aggregation or accumulation can lead to numerous neurodevelopmental and neurodegenerative disorders [5].

Our findings demonstrate that neuronal adhesion to N-cadherin extracellular domains physisorbed to the GO- or rGO-coated glass resulted in increased advection velocity of the intracellular mass in neurites relative to cells adhered to less adhesive, uncoated glass. The increased intracellular transport is possibly due to the increased regulation of the microtubule and actin cytoskeleton through cadherin-mediated adhesion. Cadherins are actin regulatory proteins and they also link to microtubules through the microtubule binding proteins PLEKHA7 and Nezha [52]. The latter interaction increases microtubule density and impacts the microtubule network [53]. Relevant to this study, the longer neurites, which were formed on N-cadherin-GO-glass and on N-cadherin-rGO-glass are indicative of stable microtubules. While receptors other than N-cadherin are also associated with microtubule formation [54], our studies suggest that surfaces coated with N-cadherin formed stable microtubules, which preferentially bind to kinesin and dynein motors [55]. In addition, increased glial cell adhesion may increase intracellular transport, possibly through the release of neurotransmitters and other extracellular signaling molecules [47].

5. Conclusion

Overall, this study demonstrated that physisorbed Fc-tagged, N-cadherin extracellular domains on GO and rGO flakes coated on glass exhibited greater average adhesive function than N-cadherin adsorbed directly to glass substrates. The increased N-cadherin-based adhesion resulted in dispersed neurons on substrates with improved intracellular mass transport along neurites. This result is attributed to concomitant increases in neurite extensions, dendritic arborization, neural network formation, and improved intracellular mass transport throughout the neural networks. These substrates thus enhance physiologically relevant neural functions *in vitro* and will facilitate future studies aimed at better understanding the development, homeostasis, and pathology of neural networks. In addition, the ability of N-cadherin-GO- and rGO-coated substrates to support single-layer neuronal cultures may facilitate drug and gene delivery studies, due to the homogeneity of the neurons in exposure to delivered drugs and genes. Furthermore, the strong coupling of cadherins between neurons with N-cadherin coated GO and rGO would thus allow for stabilization of the growth cones involved in neural pathfinding and extensions.

Author contributions

E.C.Q. and H.J.K. developed the concept and designed experiments. E.C.Q., M.E.K., and E.L. performed the experiments. E.C.Q., M.E.K., and C.K. analyzed the data. T.B.S. and C.D.K. prepared dissociated neurons. E.C.Q., D.E.L., and H.J.K. wrote the manuscript. E.C.Q., M.E.K., C.D.K., P.G., G.L.M., D.E.L., and H.J.K. edited the manuscript.

Declaration of interest

The authors declare no competing financial interest.

Acknowledgements

This work was supported by the National Science Foundation (CBET-1403491 to H.K. & D.E.L., STC-EBICS Grant CBET-0939511 to H.K., M.G., & G.P., Graduate Research Fellowship DGE – 1144245 to E.C.Q, IGERT CMMB-0965918 to E.C.Q). The authors would like to thank Dr. Scott Denmark for the use of the circular dichroism spectrometer and Saiko Rosenberger for protein purification. Experiments were carried out in part in the Frederick Seitz Materials Research Laboratory Central Research Facilities and the Carl R. Woese Institute for Genomic Biology at the University of Illinois.

Appendix A. Supplementary data

Supplementary data to this article can be found online at https://doi.org/10.1016/j.actbio.2019.04.005.

References

[1] O.I. Wagner, The interaction of neurofilaments with the microtubule motor cytoplasmic dynein, Mol. Biol. Cell. 15 (2004) 5092–5100.
[2] H. Ye, R. Kuruvilla, L.S. Zweifel, D.D. Ginty, Evidence in support of signaling endosome-based retrograde survival of sympathetic neurons, Neuron 39 (2003) 57–68.
[3] A. Kamal, A. Almenar-Queralt, J.F. LeBlanc, E.A. Roberts, L.S.B. Goldstein, Kinesin-mediated axonal transport of a membrane compartment containing β-secretase and presenilin-1 requires APP, Nature 414 (2001) 643–648.
[4] S. Gunawardena, L.S.B. Goldstein, Disruption of axonal transport and neuronal viability by amyloid precursor protein mutations in drosophila, Neuron 32 (2001) 389–401.
[5] S. Roy, B. Zhang, V.M.Y. Lee, J.Q. Trojanowski, Axonal transport defects: a common theme in neurodegenerative diseases, Acta Neuropathol. 109 (2005) 5–13.
[6] S. Millecamps, J.P. Julien, Axonal transport deficits and neurodegenerative diseases, Nat. Rev. Neurosci. 14 (2013) 161–176.
[7] T. Zech, S.D.J. Calaminus, L.M. Machesky, Actin on trafficking: could actin guide directed receptor transport?, Cell Adhes Migr. 6 (2012) 476–481.
[8] L. Bard, C. Boscher, M. Lambert, R.-M. Mege, D. Choquet, O. Thoumine, A molecular clutch between the actin flow and n-cadherin adhesions drives growth cone migration, J. Neurosci. 28 (2008) 5879–5890.

[9] Z.-J. Tan, Y. Peng, H.-L. Song, J.-J. Zheng, X. Yu, N-cadherin-dependent neuron-neuron interaction is required for the maintenance of activity-induced dendrite growth, Proc. Natl. Acad. Sci. U.S.A. 107 (2010) 9873–9878.
[10] W.J. Nelson, Regulation of cell-cell adhesion by the cadherin-catenin complex, Biochem. Soc. Trans. 36 (2008) 149–155.
[11] R. Riehl, K. Johnson, R. Bradley, G.B. Grunwald, E. Cornel, A. Lilienbaum, C.E. Holt, Cadherin function is required for axon outgrowth in retinal ganglion cells in vivo, Neuron 17 (1996) 837–848.
[12] K.J. Tomaselli, K.M. Neugebauer, J.L. Bixby, J. Lilien, L.F. Reichard, N-cadherin and integrins: two receptor systems that mediate neuronal process outgrowth on astrocyte surfaces, Neuron 1 (1988) 33–43.
[13] J.L. Bixby, J. Lilien, L.F. Reichardt, Identification of the major proteins that promote neuronal process outgrowth on schwann cells in vitro, J. Cell Biol. 107 (1988) 353–361.
[14] J.L. Bixby, R. Zhang, Purified N-cadherin is a potent substrate for the rapid induction of neurite outgrowth, J. Cell Biol. 110 (1990) 1253–1260.
[15] D.L. Benson, H. Tanaka, N-cadherin redistribution during synaptogenesis in hippocampal neurons, J. Neurosci. 18 (1998) 6892–6904.
[16] J. Arikkath, L.F. Reichardt, Cadherins and catenins at synapses: roles in synaptogenesis and synaptic plasticity, Trends Neurosci. 31 (2008) 487–494.
[17] J.X. Chia, N. Efimova, T.M. Svitkina, Neurite outgrowth is driven by actin polymerization even in the presence of actin polymerization inhibitors, Mol. Biol. Cell. 27 (2016) 3695–3704.
[18] L.D.M. Derycke, M.E. Bracke, N-cadherin in the spotlight of cell-cell adhesion, differentiation, invasion and signalling, Int. J. Dev. Biol. 48 (2004) 463–476.
[19] V. Lemmon, S.M. Burden, H.R. Payne, G.J. Elmslie, M.L. Hlavin, Neurite growth on different substrates: permissive versus instructive influences and the role of adhesive strength, J. Neurosci. 12 (1992) 818–826.
[20] B.D. Cosgrove, K.L. Mui, T.P. Driscoll, S.R. Caliari, K.D. Mehta, R.K. Assoian, J.A. Burdick, R.L. Mauck, N-cadherin adhesive interactions modulate matrix mechanosensing and fate commitment of mesenchymal stem cells, Nat. Mater. 15 (2016) 1297–1306.
[21] L. Bian, M. Guvendiren, R.L. Mauck, J.A. Burdick, Hydrogels that mimic developmentally relevant matrix and N-cadherin interactions enhance MSC chondrogenesis, Proc. Natl. Acad. Sci. U.S.A. 110 (2013) 10117–10122.
[22] M.Y. Kwon, S.L. Vega, W.M. Gramlich, M. Kim, R.L. Mauck, J.A. Burdick, Dose and timing of N-cadherin mimetic peptides regulate MSC chondrogenesis within hydrogels, Adv. Healthc. Mater. 7 (2018) 1701199.
[23] J.C.M. Vega L., M.K. Lee, J.H. Jeong, C.E. Smith, K.Y. Lee, H.J. Chung, D.E. Leckband, H. Kong, Recapitulating cell-cell adhesion using N-cadherin biologically tethered to substrates, Biomacromolecules 15 (2014) 2172–2179.
[24] J.C.M. Vega L., M.K. Lee, E.C. Qin, M. Rich, K.Y. Lee, D.H. Kim, H.J. Chung, D.E. Leckband, H. Kong, Three dimensional conjugation of recombinant N-cadherin to a hydrogel for in vitro anisotropic neural growth, J. Mater. Chem. B 4 (2016) 6803–6811.
[25] H. Tabdili, M. Langer, Q. Shi, Y.-C. Poh, N. Wang, D. Leckband, Cadherin-dependent mechanotransduction depends on ligand identity but not affinity, J. Cell Sci. 125 (2012) 4362–4371.
[26] A. González-Mayorga, E. López-Dolado, M.C. Gutiérrez, J.E. Collazos-Castro, M. L. Ferrer, F. del Monte, M.C. Serrano, Favorable biological responses of neural cells and tissue interacting with graphene oxide microfibers, ACS Omega 2 (2017) 8253–8263.
[27] R. Wang, Z. Wang, L. Millet, M.U. Gillette, A.J. Levine, G. Popescu, Dispersion-relation phase spectroscopy of intracellular transport, Opt. Express. 19 (2011) 20571.
[28] M. Mir, T. Kim, A. Majumder, M. Xiang, R. Wang, S.C. Liu, M.U. Gillette, S. Stice, G. Popescu, Label-free characterization of emerging human neuronal networks, Sci. Rep. 4 (2014) 4434.
[29] G. Popescu, Quantitative Phase Imaging of Cells and Tissues, McGraw-Hill, 2011.
[30] Z. Wang, L. Millet, V. Chan, H. Ding, M.U. Gillette, R. Bashir, G. Popescu, Label-free intracellular transport measured by spatial light interference microscopy, J. Biomed. Opt. 16 (2011) 026019.
[31] Y.J. Lee, P. Cintora, J. Arikkath, O. Akinsola, M. Kandel, G. Popescu, C. Best-Popescu, Quantitative assessment of neural outgrowth using spatial light interference microscopy, J. Biomed. Opt. 22 (2017) 066015.
[32] M.E. Kandel, D. Fernandes, A.M. Taylor, H. Shakir, C. Best-Popescu, G. Popescu, Three-dimensional intracellular transport in neuron bodies and neurites investigated by label-free dispersion-relation phase spectroscopy, Cytom. Part A 91 (2017) 519–526.
[33] Z. Wang, L. Millet, M. Mir, H. Ding, S. Unarunotai, J. Rogers, M.U. Gillette, G. Popescu, Spatial light interference microscopy (SLIM), Opt. Express. 19 (2011) 797.
[34] A. Bendali, L.H. Hess, M. Seifert, V. Forster, A.F. Stephan, J.A. Garrido, S. Picaud, Purified neurons can survive on peptide-free graphene layers, Adv. Healthc. Mater. 2 (2013) 929–933.
[35] N. Li, X. Zhang, Q. Song, R. Su, Q. Zhang, T. Kong, L. Liu, G. Jin, M. Tang, G. Cheng, The promotion of neurite sprouting and outgrowth of mouse hippocampal cells in culture by graphene substrates, Biomaterials 32 (2011) 9374–9382.
[36] V. Georgakilas, J.N. Tiwari, K.C. Kemp, J.A. Perman, A.B. Bourlinos, K.S. Kim, R. Zboril, Noncovalent functionalization of graphene and graphene oxide for energy materials, biosensing, catalytic, and biomedical applications, Chem. Rev. 116 (2016) 5464–5519.
[37] S.Y. Park, J. Park, S.H. Sim, M.G. Sung, K.S. Kim, B.H. Hong, S. Hong, Enhanced differentiation of human neural stem cells into neurons on graphene, Adv. Mater. 23 (2011) 263–267.
[38] W.C. Lee, C.H.Y.X. Lim, H. Shi, L.A.L. Tang, Y. Wang, C.T. Lim, K.P. Loh, Origin of enhanced stem cell growth and differentiation on graphene and graphene oxide, ACS Nano 5 (2011) 7334–7341.
[39] M. Lambert, F. Padilla, R.M. Mège, Immobilized dimers of N-cadherin-Fc chimera mimic cadherin-mediated cell contact formation: contribution of both outside-in and inside-out signals, J. Cell Sci. 113 (2000) 2207–2219.
[40] A.K. Prakasam, V. Maruthamuthu, D.E. Leckband, Similarities between heterophilic and homophilic cadherin adhesion, Proc. Natl. Acad. Sci. 103 (2006) 15434–15439.
[41] C. Mattevi, G. Eda, S. Agnoli, S. Miller, K.A. Mkhoyan, O. Celik, D. Mastrogiovanni, G. Granozzi, E. Carfunkel, M. Chhowalla, Evolution of electrical, chemical, and structural properties of transparent and conducting chemically derived graphene thin films, Adv. Funct. Mater. 19 (2009) 2577–2583.
[42] D.K. Owens, R.C. Wendt, Estimation of the surface free energy of polymers, J. Appl. Polym. Sci. 13 (1969) 1741–1747.
[43] A. Das, B. Chakraborty, A.K. Sood, Raman spectroscopy of graphene on different substrates and influence of defects, Bull. Mater. Sci. 31 (2008) 579–584.
[44] A.W. Koch, D. Bozic, O. Pertz, J. Engel, homophilic adhesion by cadherins, Curr. Opin. Struct. Biol. 9 (1999) 275–281.
[45] Q. Shi, Y.-H. Chien, D. Leckband, Biophysical properties of cadherin bonds do not predict cell sorting, J. Biol. Chem. 283 (2008) 28454–28463.
[46] S. Kaech, G. Banker, Culturing hippocampal neurons, Nat. Protoc. 1 (2006) 2406–2415.
[47] R.D. Fields, B. Stevens-Graham, New insights into neuron-glia communication, Science 298 (2002) 556–562.
[48] B.A. Barres, The mystery and magic of Glia: a perspective on their roles in health and disease, Neuron 60 (2008) 430–440.
[49] H.R. Payne, V. Lemmon, Glial cells of the O-2A lineage bind preferentially to N-cadherin and develop distinct morphologies, Dev. Biol. 159 (1993) 595–607.
[50] P. Pittet, K. Lee, A.J. Kulik, J.-J. Meister, B. Hinz, Fibrogenic fibroblasts increase intercellular adhesion strength by reinforcing individual OB-cadherin bonds, J. Cell Sci. 121 (2008) 877–886.
[51] N. Hirokawa, Y. Noda, Y. Tanaka, S. Niwa, Kinesin superfamily motor proteins and intracellular transport, Nat. Rev. Mol. Cell Biol. 10 (2009) 682–696.
[52] W. Meng, Y. Mushika, T. Ichii, M. Takeichi, Anchorage of microtubule minus ends to adherens junctions regulates epithelial cell-cell contacts, Cell 135 (2008) 948–959.
[53] A. Chausovsky, A.D. Bershadsky, G.G. Borisy, Cadherin-mediated regulation of microtubule dynamics, Nat. Cell Biol. 2 (2000) 797–804.
[54] A.F. Palazzo, C.H. Eng, D.D. Schlaepfer, E.E. Marcantonio, G.G. Gundersen, Localized stabilization of microtubules by integrin- and FAK-facilitated rho signaling, Science 303 (2004) 836–839.
[55] A. Kamal, L.S. Goldstein, Connecting vesicle transport to the cytoskeleton, Curr. Opin. Cell Biol. 12 (2000) 503–508.

Please cite this article as: E. C. Qin, M. E. Kandel, E. Liamas et al., Graphene oxide substrates with N-cadherin stimulates neuronal growth and intracellular transport, Acta Biomaterialia, https://doi.org/10.1016/j.actbio.2019.04.005